GO-CNTs hybrids reinforced epoxy composites with porous structure as microwave absorbers

Yu Liu, Delong He, Olivier Dubrunfaut, Anne Zhang, Hanlu Zhang, Lionel Pichon, Jinbo Bai

GO-CNTs hybrids reinforced epoxy composites with porous structure as microwave absorbers

Yu LIU[1], Delong HE[1], Olivier DUBRUNFAUT[2], Anne ZHANG[1], Hanlu ZHANG[1], Lionel PICHON[2]*, Jinbo BAI[1]*

1. Université Paris-Saclay, CentraleSupélec, CNRS, Laboratoire de Mécanique des Sols, Structures et Matériaux (MSSMat), 91190, Gif-sur-Yvette, France

2. Université Paris-Saclay, CentraleSupélec, CNRS, Sorbonne Université, Laboratoire Génie électrique et électronique de Paris (GeePs), 91190, Gif-sur-Yvette, France

*** Corresponding author:**

Dr. Jinbo Bai, Email: jinbo.bai@centralesupelec.fr.

Dr. Lionel Pichon, Email: lionel.pichon@centralesupelec.fr

Abstract

Foam structures with epoxy as matrix and both carbon nanotubes (CNTs) and their hybrids with graphene oxide (GO-CNTs) as absorber were fabricated, and their microwave absorbing and electromagnetic properties were investigated in the frequency range of 1-18 GHz. The fillers and bubbles were uniformly distributed in the composites. The complex permittivity and electrical conductivity of the composites increased as the fillers' content increasing. The best performance of the reflection loss (RL) can be obtained for a foam structure with 0.5 wt% GO-CNTs, which had a RL peak value of -20dB with a -10 dB range of 5.3 GHz (10.8-16.1 GHz). Multi-layered structures were also discussed in this work, a RL peak value of -40dB with a -10dB range of 7.1GHz (9.9-17GHz) have been obtained by combining two foam structures, which are 2 mm thick 0.5 wt% GO-CNTs/epoxy and 1mm thick 2.0 wt% GO-CNTs/epoxy. Furthermore, the -10dB range can reach 11.5GHz (6.5-18GHz) when combining 2.6mm thick 0.5 wt% GO-CNTs/epoxy and 1.3mm thick 2.0 wt% GO-CNTs/epoxy.

Key words: Carbon nanotubes; Hybrid composites; Layered structures; Microwave absorber

1 Introduction

Over the last decades, broadband, thin, and lightweight electromagnetic (EM) absorbers are getting increasing interest in both civil and military applications [1-3]. Incorporating magnetic or dielectric fillers into polymer matrix is an efficient way to form composite absorbers [4-10]. Many different types of fillers have been developed. Among them, carbon nanotubes (CNTs) are the ideal materials for microwave absorption and electromagnetic interference (EMI) shielding applications due to their excellent physical and chemical properties [11-14].

However, CNTs have large surface area and tend to aggregate due to the Van der Waals force, which makes CNTs very difficult to be homogeneously dispersed in polymers. Many methods have been developed in order to improve CNT dispersibility in the matrix, which can be divided into two categories: modifying the structure of CNTs and improving the dispersion method [15, 16]. Ultrasonic, mechanical stirring and three-roll milling are three most used dispersion methods. By prolonging the processing time or increasing the stirring speed or ultrasonic power, the nanotube dispersion can be improved. Also, many methods concerning CNT surface modification have been reported in the literature to improving their dispersibility, such as oxidation. However, these methods may destroy the intrinsic properties of CNTs, e.g. the electrical conductivity of CNTs will be decreased largely after oxidation [17]. Growing CNTs on 2D nanoparticles to form hybrids became a promising method to achieve a homogeneous dispersion [18, 19]. Graphene-based 2D materials have been attracted enormous attention due to their excellent properties [20]. Liao et al. fabricated CNTs-graphene oxide/polyimide composite, which showed high dielectric permittivity and enhanced thermal stability [21]. In our previous work, a hybrid (GO-CNTs) constructed by graphene oxide (GO) and CNTs has been fabricated by the chemical vapor deposition method (CVD), which formed a 3D structure by combining the 1D CNT and 2D graphene. Such hybrids maintained the intrinsic properties of CNTs, and can help to disperse the CNTs in the matrix [22, 23].

An ideal EM wave absorber should have several merits, such as strong electromagnetic wave absorption efficiency, wide absorption band width, low density and thin material thickness. Usually, the reflection loss of CNT-based polymer composites can achieve a very high value. However, the further applications of the CNT-based polymer composites were limited by the large material thickness and narrow effective absorption band width. To overcome these problems, several meaningful works have already been done. Among them, developing multi-layered and porous structure is one of the most effective methods [24-26]. Undoubtedly, the porous or hollow structure can lower the composite density and enhance the absorption behavior by increasing the multi-reflecting and scattering percentage [27]. The multi-layered structure has been proved to be effective in terms of achieving the impedance matching condition [28].

In this paper, Epoxy has been employed as the matrix, which is a widely used thermoset plastic materials [29]. the composites reinforced by the GO-CNTs hybrid and CNTs were fabricated. The dielectric

properties and microwave absorption performance were investigated. To further improve the absorption performance, Azobisisobutyronitrile (AIBN) was used to form porous structures during curing. Based on the dielectric properties of the composites, we designed a double-layered absorption structure and simulated the corresponding absorption performance.

2 Experiments

2.1 Materials

CNTs and GO were bought from Nanocyl Science Inc., Belgium, and GRAPHENE STANDRAD, Korea, respectively. They were used directly without further treatment. Tetraethyl orthosilicate (TEOS) and Azobisisobutyronitrile (AIBN) were bought from Sigma Aldrich. Epoxy resin (bisphenol F-(epichlorhydrin)) and curing agent (4-4'-methylenebis (cyciohexylamine)) were bought from Resoltech Ltd., France.

2.2 Samples preparation

The GO-CNTs hybrids were fabricated by a one-step CVD method. More details can be found in our previous work [22]. The 1.0 wt% CNTs/epoxy foam structure was fabricated as shown in **Figure 1**. In detail: 0.06g CNTs was added into 4.5 g of epoxy resin by vigorously stirring for 10 min to obtain a homogeneous suspension. Afterwards, 1.5 g curing agent and 0.6 g AIBN were added into the previous sample. Then, the mixture was poured into an aluminum mold with a thickness of 1 mm. After degassed for 60 min at room temperature in a vacuum oven, the sample was cured at 60°C for 16 h. Finally, the sample was annealed at 100°C for 1h to complete the fully decomposition of AIBN. The same procedure was applied on GO-CNTs /epoxy foam structures. The solid CNTs/epoxy composites were fabricated by the same process without adding the AIBN to make a comparison. For each type of composites, four contents, 0.5 wt%, 1.0 wt%, 2.0 wt% and 3.0 wt%, have been prepared, respectively.

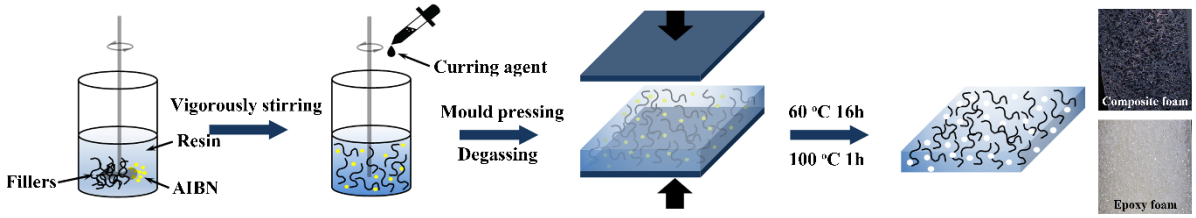

Figure 1 Schematic for the fabrication of composite foams.

2.3 Characterization

The nanofillers morphology and the composite fracture surface were characterized by the scanning electron microscope (SEM, LEO 1530 Gemini). The nanofillers were also characterized by the transmission electron microscope (TEM, TITAN G2 60-300). The carbon structure of the nanofillers was evaluated by the Raman Spectrometer (LabRAM HORIBA Jobin Yvon, Edison, NJ, USA) at room

temperature. The permittivity of the composites was measured by a network analyzer (Keysight E8364C) at room temperature. The standard of the guide used was APC 7mm. The sample was polished to a round with a diameter of 7mm and settled between a short-circuit and a coaxial waveguide, as shown in **Figure 2**. The reflection coefficient measured was calculated with an analytical method to obtain the complex permittivity [30].

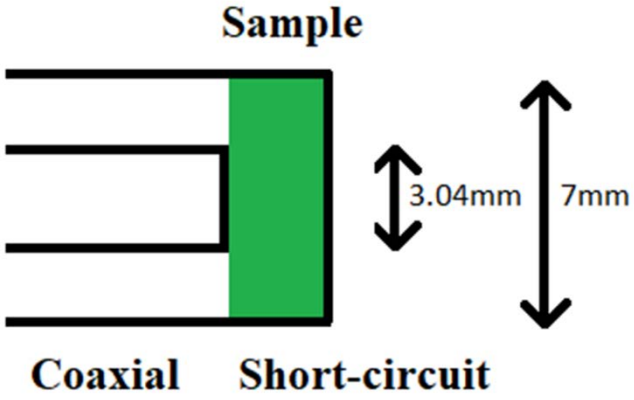

Figure 2 Geometry for high frequency test.

3 Results and discussion

3.1 Morphology and structure of the nano-fillers and epoxy composites

The CNTs was grown on the GO surface by CVD method. The ferrocene was used as the catalyst precursor. **Figure 3A** showed the hybrids fabricated by CVD with synthesis time of 5 min. All the GO platelets have been covered by the vertical CNT clusters. The length and diameter of CNTs grown on the platelet surface were uniform with the length of about 5 μm and the diameter in the range of 10-20 nm, respectively. The edge of GO platelet was obvious in the hybrids. **Figure 3B** showed the hybrids by CVD with synthesis time of 10 min. After prolonging the synthesis time, the CNTs was longer and much denser on the GO platelets. The detailed structure was further revealed by TEM. **Figure 3C** presents the high resolution TEM image of CNTs, which has a diameter of around 20 nm. Comparing to the TEM image of hybrids (**Figure 3D**), it can be found that the CNTs in the hybrids have more regular structure than the Nanocyl CNTs.

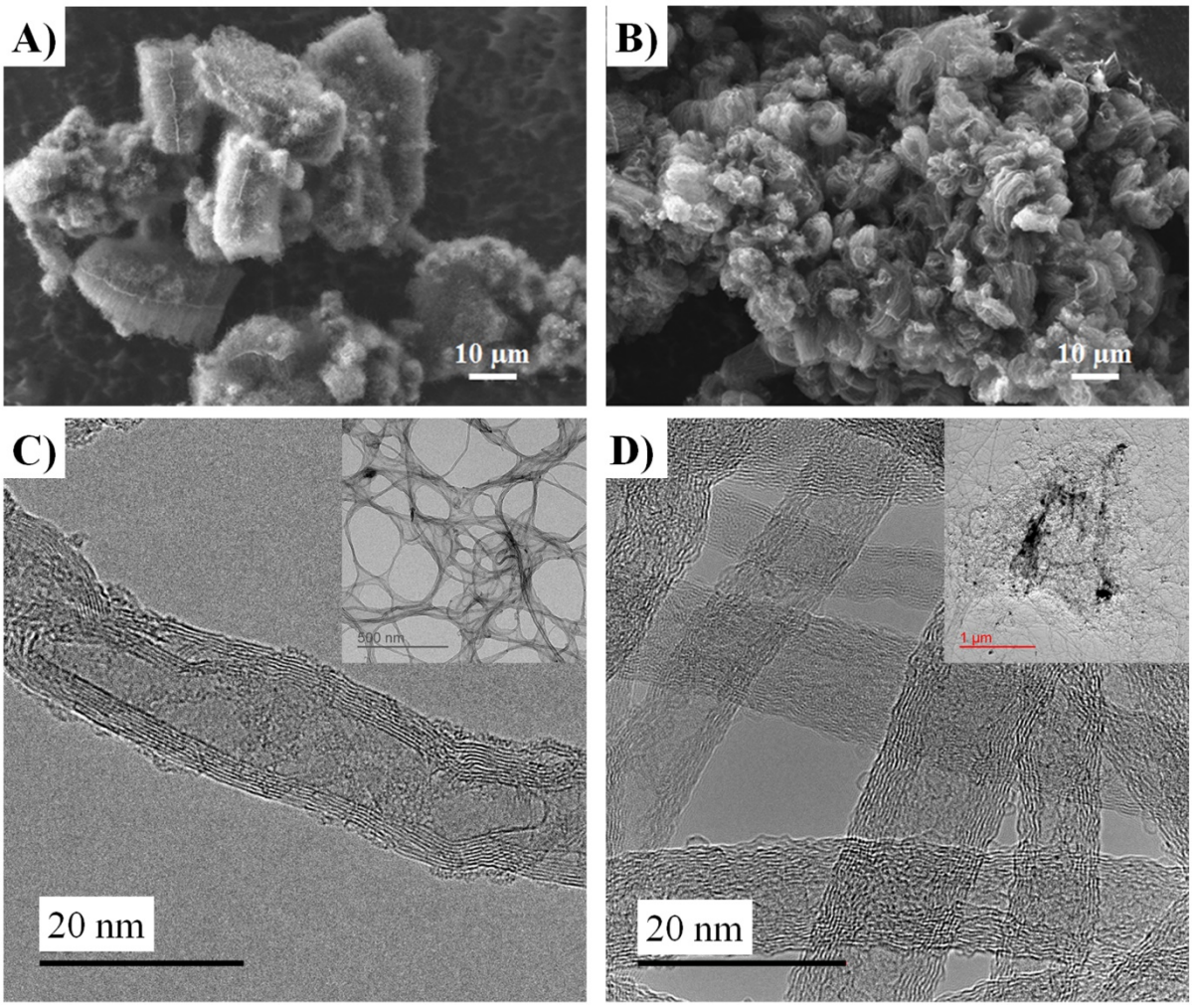

Figure 3 SEM images of (A) GO-CNTs with synthesis time of 5 min; (B) GO-CNTs with synthesis time of 10 min; TEM images of (C) CNTs and (D) GO-CNTs hybrids.

Figure 4 presented Raman spectra of CNTs and GO-CNTs hybrids. Two typical peaks appeared on the spectra, 1330 cm^{-1} and 1598 cm^{-1} corresponding to the D band and tangential G band respectively. The CNTs and GO-CNTs hybrids had almost the same Raman spectra, indicating that they have the similar structures of CNTs, since the CNTs possessed most part in the hybrids.

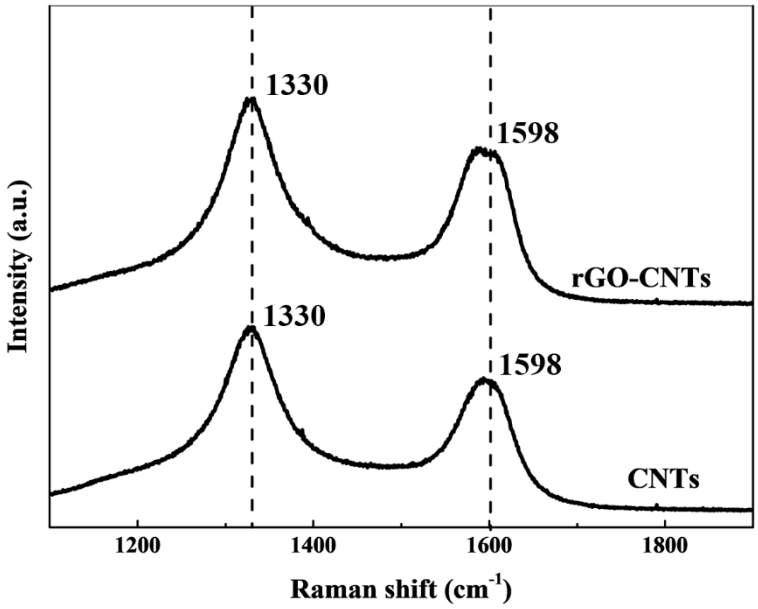

Figure 4 Raman spectra of CNTs and hybrids.

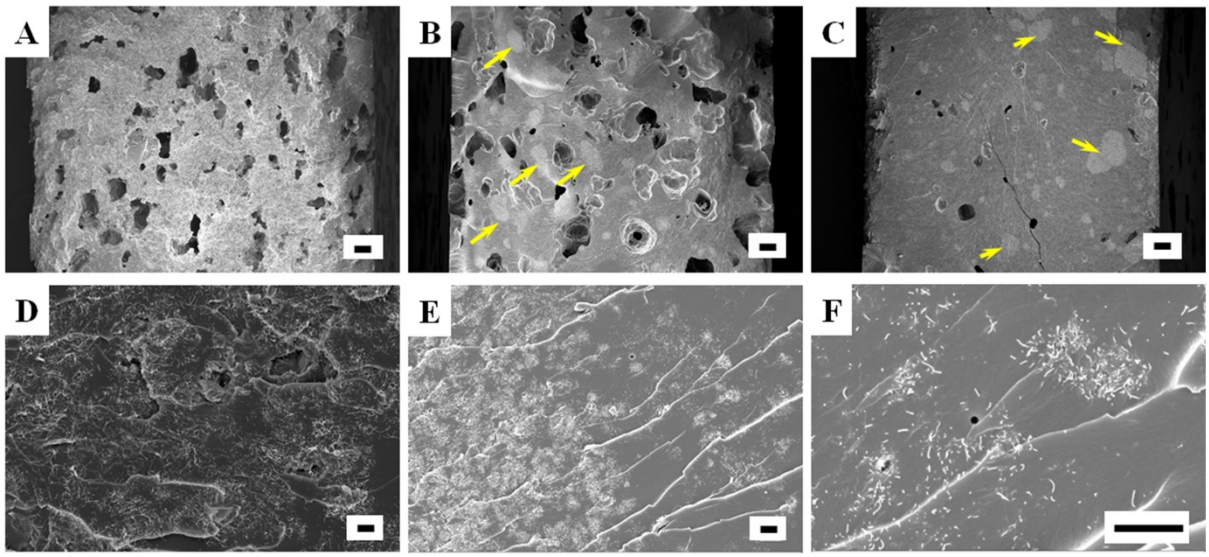

Figure 5 SEM images of the cross-section of 3.0 wt% foam and solid composites: (A) and (D) showed the 3.0 wt% GO-CNTs/epoxy foam composite; (B), (E) and (F) showed the 3.0 wt% CNTs/epoxy foam composite; (C) shows the 3.0 wt% CNTs/epoxy solid composites. (The length of the scale bar in Figure 4A, 4B and 4C was 100 μm. The length of scale bar in Figure 4D, 4E and 4F was 2μm.)

Figure 5 showed the SEM images of the cross-section morphology of epoxy composites with solid and foam structures. **Figure 5A** was the cross section of the 3.0 wt % GO-CNTs/epoxy foam composite. It can be found that large number of pores were appeared throughout the GO-CNTs/epoxy system, which showed the irregular shape with the sizes ranged from 50 to 100 μm. The pores were formed by adding AIBN into the composites, which decomposed at high temperature and released a large volume of nitrogen gas. The AIBN distributed homogeneously in the resin by vigorously stirring. After

decomposing at high temperature, the released gas formed pores in the cured matrix, and generated a GO-CNTs/epoxy foam structure. The irregular shape of the bubbles was due to the high viscosity of the un-cured matrix filled with 3.0 wt% GO-CNTs, which was a relatively high content for the CNT-based composite. **Figure 5D** showed a high magnification SEM image, it can be clearly seen that the GO-CNTs hybrids were distributed homogeneously in the epoxy matrix and formed an interconnected CNT network, which may build an electrically conductive network in the matrix. **Figure 5B** and **5C** showed the morphology of the foam and solid structures of 3.0 wt% CNTs/epoxy composites, respectively. The CNTs/epoxy foam structure had the similar morphology as the GO-CNTs/epoxy foam structure. However, the dispersion of CNTs was worse than that of the GO-CNTs hybrids. After vigorously stirring, the CNT clusters still appeared in the matrix, as marked out by the arrows. At shown in the high magnification image (**Figure 5E** and **5F**), the aggregations were consisted by the small clusters of CNTs, even in the region out of aggregations, the CNTs distribution was not uniform. There existed several bubbles in the solid CNTs/epoxy composites, which were due to the high viscosity of the matrix, the bubbles were difficult to run away from the uncured matrix.

3.2 Effect of the mass fraction of nano-fillers on the complex permittivity and conductivity of the epoxy composites

In order to study the electromagnetic properties of the composites, the complex permittivity and conductivity of the composites were measured in the frequency range of 1–18 GHz. The complex permittivity and conductivity spectra of the composites containing GO-CNTs and CNTs were shown in **Figure 6**. The real (ε′) and imaginary (ε″) part of complex permittivity of the composites increased as the fraction of the nano-fillers increased from 0.5 to 3.0 wt%. The highest values of the ε′ of the solid and foam composite filled with 3.0 wt% CNTs and GO-CNTs reached to 54, 38 and 55, respectively. The highest values of the ε″ of the solid and foam composites filled with 3.0 wt% CNTs and GO-CNTs reached to 84, 40 and 81, respectively. As the frequency increased, the complex permittivity tended to decrease. Usually, the dielectric properties of the composites depend on the dispersion, the mass content of the nano-fillers, and the configuration of the composites. Based on the analysis, GO-CNTs/epoxy composites had better dielectric properties than the CNTs/epoxy composites, especially at low mass contents, which was due to the easier and better dispersion of hybrids in the matrix. Comparing the foam structures with the solid structure filled with CNTs, the solid structure had better performance than the foam one, which was reasonable since the foam structure had less effective CNTs to form the conductive network in the matrix due to the existence of bubbles. The conductivity was then deduced:

$$\sigma_{AC} = \sigma'(\omega) = \varepsilon_0 \varepsilon'' \omega \qquad (1)$$

As the frequency increased, the conductivity tended to increase.

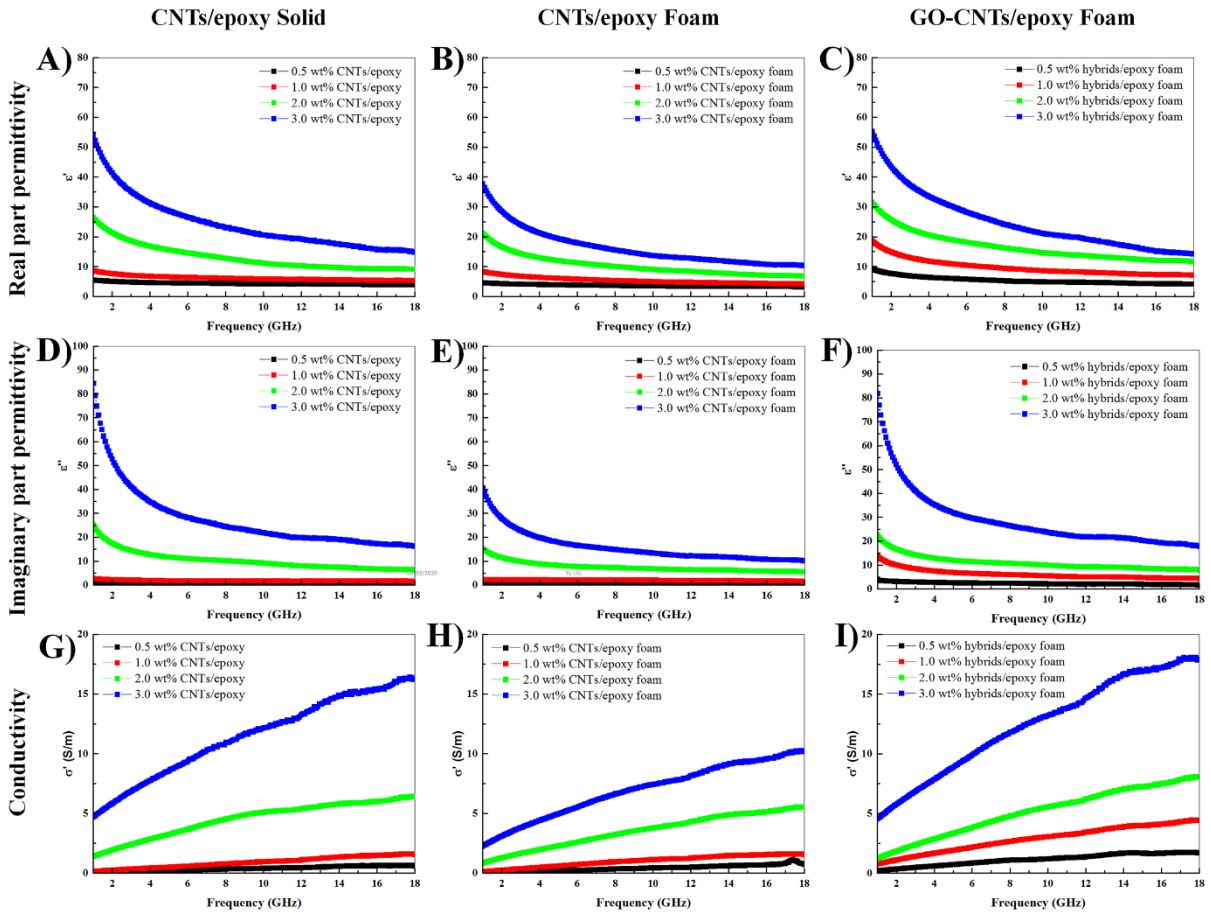

Figure 6 Real part permittivity of (A) CNTs/epoxy solid composite, (B) CNTs/epoxy foam composite and (C) GO-CNTs/epoxy foam composite; Imaginary part permittivity of (D) CNTs/epoxy solid composite, (E) CNTs/epoxy foam composite and (F) GO-CNTs/epoxy foam composite; and Conductivity of (G) CNTs/epoxy solid composite, (H) CNTs/epoxy foam composite and (I) GO-CNTs/epoxy foam composite as a function of frequency.

3.3 The microwave absorption of nano-fillers reinforced epoxy composites with solid and foam structures

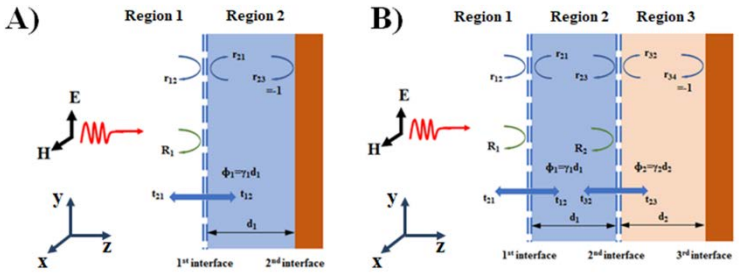

Figure 7 (A) Single-layered and **(B)** double-layered electromagnetic wave absorber.

As shown in **Figure 7A**, an electromagnetic plane wave was perpendicularly incident into a single-layered absorber along the in z-direction. The total reflection coefficient could be expressed as [31]

$$R_1 = r_{12} + \frac{t_{21}t_{12}r_{23}e^{-2i\Phi_1}}{1-r_{21}r_{23}e^{-2i\Phi_1}} \qquad (2)$$

Where r_{ij} was the individual reflection coefficient and t_{ij} was the represent individual transmission coefficient. The back plane was considered as a perfect reflector, i.e., $r_{23} = -1$. $\Phi_1 = \gamma_1 d_1$ was the phase lengths across the dielectric substrates, where d_1 was the material thickness, γ_1 was the complex propagation constant. The r_{ij} and t_{ij} had a relationship as $t_{ij}=1+r_{ij}$, r_{ij} and r_{ji} were opposite numbers. Hence, the equation (2) can be simplified as

$$R_1 = \frac{r_{12}-e^{-2i\Phi_1}}{1-r_{12}e^{-2i\Phi_1}} \qquad (3)$$

And

$$r_{12} = \frac{\eta_2-\eta_1}{\eta_2+\eta_1} \qquad (4)$$

Where

$$\eta_1 = \sqrt{\frac{\mu_1}{\varepsilon_1}}\left(1 - j\frac{\sigma_1}{\omega\varepsilon_1}\right)^{-\frac{1}{2}} \qquad (5)$$

$$\eta_2 = \sqrt{\frac{\mu_2}{\varepsilon_2}}\left(1 - j\frac{\sigma_2}{\omega\varepsilon_2}\right)^{-\frac{1}{2}} \qquad (6)$$

ε_1 and ε_2 were absolute permittivity, ε_1 and ε_2 were in F/m.

For air, $\sigma_1 \to 0$, hence,

$$\eta_1 = \sqrt{\frac{\mu_0}{\varepsilon_0}} \qquad (7)$$

Where μ_2 was the permeability of the region 2, μ_0 was the vacuum permeability and ε_0 was the vacuum permittivity.

If the absorber was a double-layered structure as shown in **Figure 7B**, the total reflection coefficient on the first and second interface could be expressed as [31]:

$$R_1 = r_{12} + \frac{t_{21}t_{12}R_2e^{-2i\Phi_1}}{1-r_{21}R_2e^{-2i\Phi_1}} \qquad (8)$$

$$R_2 = r_{23} + \frac{t_{32}t_{23}r_{34}e^{-2i\Phi_2}}{1-r_{32}r_{34}e^{-2i\Phi_2}} \qquad (9)$$

Which could also be simplified as

$$R_1 = \frac{r_{12}+R_2 e^{-2i\Phi_1}}{1+r_{12}R_2 e^{-2i\Phi_1}} \qquad (10)$$

$$R_2 = \frac{r_{23}-e^{-2i\Phi_2}}{1-r_{23}e^{-2i\Phi_2}} \qquad (11)$$

And the reflection loss of single layer or double layers could be expressed as

$$R_L = -20\lg|R_1| \qquad (12)$$

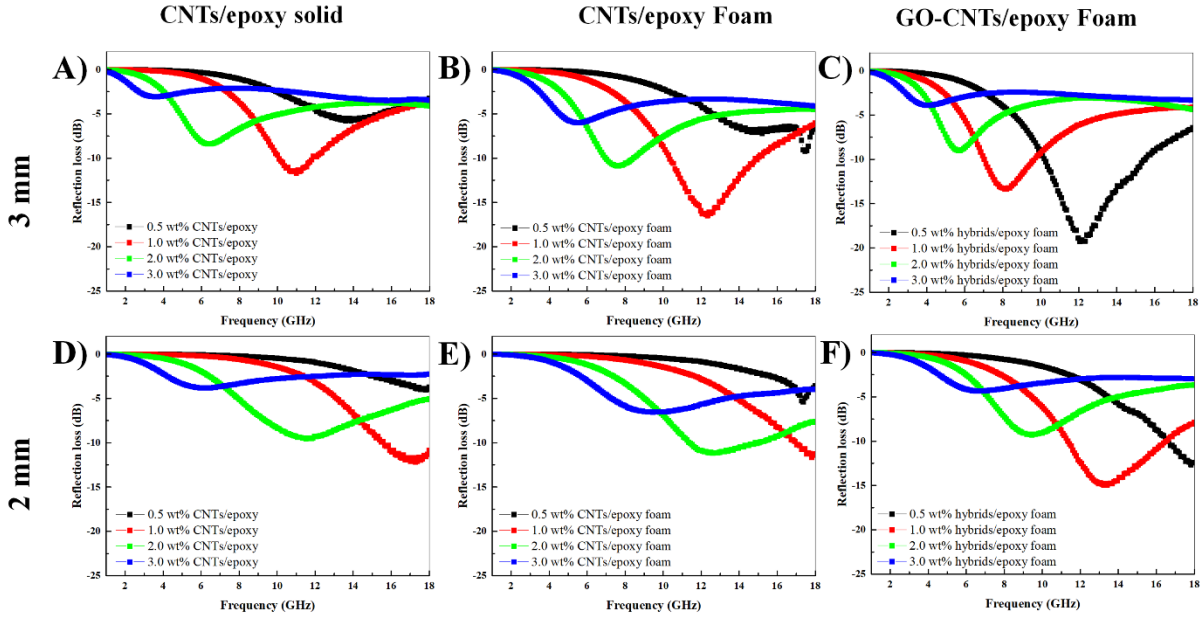

Figure 8 The reflection loss of the composites with different content of fillers varied from 0.5 wt% to 3.0 wt% with different thickness as a function of frequency: (A) CNTs/epoxy solid structures 3mm; (B) CNTs/epoxy foam structures 3mm and (C) GO-CNTs/epoxy foam structures 3mm; (D) CNTs/epoxy solid structures 2mm; (E) CNTs/epoxy foam structures 2mm and (F) GO-CNTs/epoxy foam structures 2mm.

Figure 8 showed the reflection loss of the epoxy composite containing 0.5 wt% to 3.0 wt% nano-fillers with different thickness. For all three composites, as the fraction of fillers increased, the absorption peaks were shifted to the low frequency region. For the 1.0 wt% CNTs/epoxy solid composites with 3mm in thickness, the effective absorption bandwidth (-10 dB) was only 1.8 GHz (10.0-11.8 GHz). The effective absorption bandwidth can reach 4.6 GHz (10.3–14.9 GHz) for the 1.0 wt% CNTs/epoxy foam structures with 3mm in thickness. The GO-CNTs/epoxy foam composites with 3mm in thickness have the best performance, and the effective absorption bandwidth can achieve 5.2 GHz (10.3–15.5 GHz) with the content of only 0.5 wt%.

Based on the impedance matching condition, the impedance matching degree highly depended on the complex permittivity. The corresponding attenuation constant (α) and input impedance (Z_{in}) can be obtained based on the equations [32]:

$$Z_{in} = Z_0\sqrt{\frac{\mu_r}{\varepsilon_r}}\tanh\left(j\frac{2\pi fd}{c}\sqrt{\mu_r\varepsilon_r}\right) \qquad (13)$$

$$\alpha = \frac{\sqrt{2}\pi f}{c}\sqrt{(\mu''\varepsilon'' - \mu'\varepsilon') + \sqrt{(\mu''\varepsilon'' - \mu'\varepsilon')^2 + (\mu'\varepsilon'' - \mu''\varepsilon')^2}} \qquad (14)$$

Where c was the light speed, d was the sample thickness, ε' and ε'' were the real part and imaginary part of permittivity, and μ' and μ'' were the real part and imaginary part of permeability. μ_r and ε_r were the relative permeability and permittivity, respectively.

The impedance of vacuum (Z_0) was 377Ω. For nonmagnetic materials, μ'=1 and μ''=0, hence, the attenuation constant could be simplified as

$$\alpha = \frac{\sqrt{2}\pi f}{c}\sqrt{\sqrt{(\varepsilon')^2 + (\varepsilon'')^2} - \varepsilon'} \qquad (15)$$

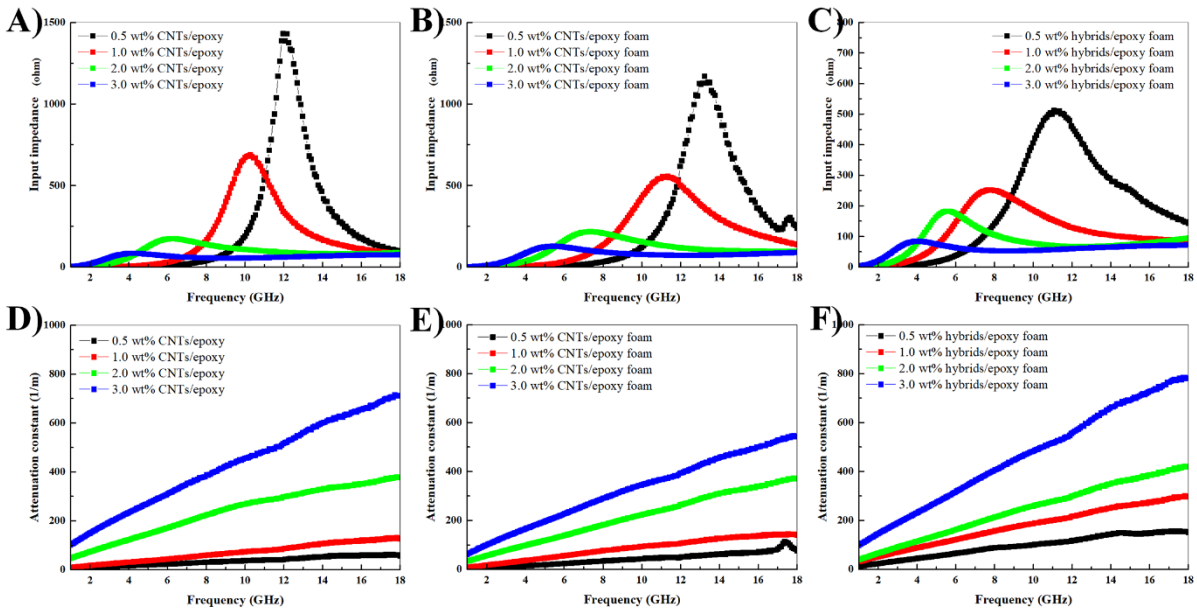

Figure 9 The input impedance of (A) CNTs/epoxy solid structures, (B) CNTs/epoxy foam structures and (C) GO-CNTs/epoxy foam structures with the thickness of 3mm; The attenuation constant of (D) CNTs/epoxy solid structures, (E) CNTs/epoxy foam structures and (F) GO-CNTs/epoxy foam structures.

The electromagnetic wave can easily penetrate into the material when the impedance of composite closed to that of the vacuum, which was 377Ω. After the electromagnetic wave enters the materials, a good absorption performance can be obtained when the material has a high attenuation constant. **Figure 9** showed the input impedance and the attenuation constant the composites with 3mm in thickness. The input impedance decreased following the increase of filler contents for the three types of composites. In the tested frequency range (1-18GHz), the closest input impedance to the vacuum are 1.0 wt% CNTs/epoxy solid structure, 1.0 wt% CNTs/epoxy foam structure and 0.5 wt% GO-CNTs/epoxy foam structure, respectively. The attenuation constant increased with the increase of filler contents. Within

the three composites mentioned above, 0.5 wt% GO-CNTs/epoxy foam structure has the highest attenuation constant, which leads to a best performance of the reflection loss.

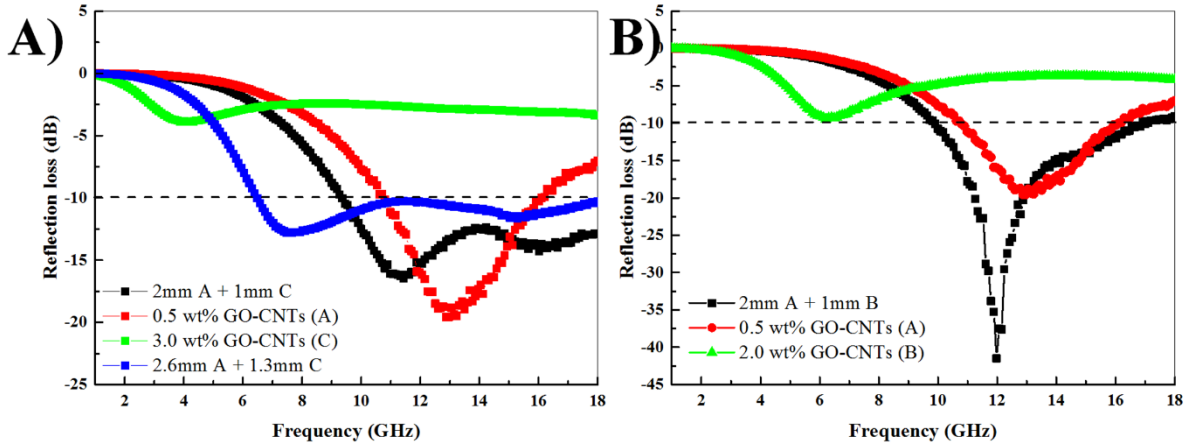

Figure 10 Optimized double layered structures for the specific requirement: (A) the widest frequency range of -10 dB and (B) the lowest refection loss in the tested frequency range. All the sample thicknesses were 3mm except the blue line which had the widest frequency range of -10 dB, and its thickness was 3.9mm.

A double-layered structure, containing an impedance layer and an absorption layer, can largely improve the absorption properties. In this work, the 0.5 wt% GO-CNTs/epoxy foam structure was selected as the impedance layer, and the 3.0 wt% GO-CNTs/epoxy foam structure was selected as the absorption layer due to the high attenuation constant as well as the high complex permittivity. When the thickness of impedance layer was 2.0 mm, and the thickness of absorption layer was 1.0 mm, the peak value of RL decreased to about 15 dB, but the effective absorption bandwidth was 8.7 GHz (9.3-18 GHz), as shown in **Figure 10A**. When the impedance layer increased to 2.6 mm, and the absorption layer increased to 1.3 mm, the peak value of RL decreased to about 12.8 dB, but the effective absorption bandwidth can reach 11.5 GHz (6.5-18GHz). When the 2.0 wt% GO-CNTs/epoxy foam structure was selected as the absorption layer, the peak value of RL could reach -41.5 dB with the effective absorption bandwidth of 7.1 GHz (9.9-17 GHz), as shown in **Figure 10B**. In Table 1, we have listed some similar studies. The double-layered structure simulated in this work was competitive can be fabricated with good absorbing properties.

Table 1 Some similar studies about absorption structures.

Samples	Layers	Filler contents (wt%)	RL (dB)	Bandwidth (GHz) (<-10 dB)	Thickness (mm)	Reference
CB/SiO_{2f}/polyimide	Double	5+15	-29.5	2.75	3	[33]
Ag coated glass fiber	Double	--	-32.3	2.84	1.84	[34]
CNTs/SiCf/polyimid	Double	1+3	-29.8	2.18	3.0	[35]
GO-CNTs/epoxy foam	Double	0.5+3	-12.8	11.5	3.9	This work
		0.5+2	-41.5	7.1	3.0	

4 Conclusion

The GO-CNTs hybrids have been successfully fabricated by a one-step CVD method. Microwave absorbing foam structures with epoxy as matrix and both CNTs and GO-CNTs as absorber were prepared by using AIBN as the pore creating agent, and their electromagnetic and microwave absorbing properties were investigated in the frequency range of 1–18 GHz. The complex permittivity and electrical conductivity of the composites increased with increasing fillers' content. A best performance of the reflection loss can be obtained for a foam structure with 0.5 wt% GO-CNTs, which had a peak value of -20dB with a -10dB range of 5.3 GHz (10.8-16.1 GHz). Then, the influence of input impedance and attenuation constant on the absorption performance was also discussed. Based on this result, the double-layered structure was designed. A peak value of -40dB with a -10dB range of 7.1GHz (9.9-17GHz) can be obtained by combining two foam structures, which are 2mm 0.5 wt% GO-CNTs and 1mm 2.0 wt% GO-CNTs. Furthermore, the -10dB range can reach 11.5GHz (6.5-18GHz) if combining 2.6mm 0.5 wt% GO-CNTs and 1.3mm 2.0 wt% GO-CNTs.

Acknowledgments

This work has benefited from the financial support of the LabEx LaSIPS, France (ANR-10-LABX-0032-LaSIPS) managed by the French National Research Agency under the ''Investissements d'avenir'' program (ANR-11-IDEX-0003).

References

[1] J. Choi, H.-T. Jung, A new triple-layered composite for high-performance broadband microwave absorption, Composite Structures, 122 (2015) 166-171.
[2] S. Xia, B. Yao, Q. Chen, X. Yu, Q. Wu, Composites with Koch fractal activated carbon fiber felt screens for strong microwave absorption, Composites Part B: Engineering, 105 (2016) 1-7.
[3] L. Zhang, C. Shi, K.Y. Rhee, N. Zhao, Properties of Co0.5Ni0.5Fe2O4/carbon nanotubes/polyimide nanocomposites for microwave absorption, Composites Part A: Applied Science and Manufacturing, 43 (2012) 2241-2248.
[4] R. Ji, C. Cao, Z. Chen, H. Zhai, J. Bai, Solvothermal synthesis of CoxFe3−xO4 spheres and their microwave absorption properties, Journal of Materials Chemistry C, 2 (2014) 5944-5953.
[5] Q. Liu, X. Xu, W. Xia, R. Che, C. Chen, Q. Cao, J. He, Dependency of magnetic microwave absorption on surface architecture of Co20Ni80 hierarchical structures studied by electron holography, Nanoscale, 7 (2015) 1736-1743.
[6] A. Shah, Y. Wang, H. Huang, L. Zhang, D. Wang, L. Zhou, Y. Duan, X. Dong, Z. Zhang, Microwave absorption and flexural properties of Fe nanoparticle/carbon fiber/epoxy resin composite plates, Composite Structures, 131 (2015) 1132-1141.
[7] A.A. Al-Ghamdi, O.A. Al-Hartomy, F.R. Al-Solamy, N. Dishovsky, P. Malinova, G. Atanasova, N. Atanasov, Conductive carbon black/magnetite hybrid fillers in microwave absorbing composites based on natural rubber, Composites Part B: Engineering, 96 (2016) 231-241.

[8] J. Hu, T. Zhao, X. Peng, W. Yang, X. Ji, T. Li, Growth of coiled amorphous carbon nanotube array forest and its electromagnetic wave absorbing properties, Composites Part B: Engineering, 134 (2018) 91-97.
[9] H. Zhang, J. Zhang, H. Zhang, Electromagnetic properties of silicon carbide foams and their composites with silicon dioxide as matrix in X-band, Composites Part A: Applied Science and Manufacturing, 38 (2007) 602-608.
[10] R. Shu, Y. Wu, W. Li, J. Zhang, Y. Liu, J. Shi, M. Zheng, Fabrication of ferroferric oxide–carbon/reduced graphene oxide nanocomposites derived from Fe-based metal–organic frameworks for microwave absorption, Composites Science and Technology, 196 (2020) 108240.
[11] T.L. Makarova, P. Geydt, I. Zakharchuk, E. Lahderanta, A.A. Komlev, A.A. Zyrianova, M.A. Kanygin, O.V. Sedelnikova, V.I. Suslyaev, L.G. Bulusheva, A.V. Okotrub, Correlation between manufacturing processes and anisotropic magnetic and electromagnetic properties of carbon nanotube/polystyrene composites, Composites Part B: Engineering, 91 (2016) 505-512.
[12] Y. Liu, D. Song, C. Wu, J. Leng, EMI shielding performance of nanocomposites with MWCNTs, nanosized Fe3O4 and Fe, Composites Part B: Engineering, 63 (2014) 34-40.
[13] J.R.N. Gnidakouong, M. Kim, H.W. Park, Y.-B. Park, H.S. Jeong, Y.B. Jung, S.K. Ahn, K. Han, J.-M. Park, Electromagnetic interference shielding of composites consisting of a polyester matrix and carbon nanotube-coated fiber reinforcement, Composites Part A: Applied Science and Manufacturing, 50 (2013) 73-80.
[14] R. Shu, Y. Wu, Z. Li, J. Zhang, Z. Wan, Y. Liu, M. Zheng, Facile synthesis of cobalt-zinc ferrite microspheres decorated nitrogen-doped multi-walled carbon nanotubes hybrid composites with excellent microwave absorption in the X-band, Composites Science and Technology, 184 (2019) 107839.
[15] J.A. Kim, D.G. Seong, T.J. Kang, J.R. Youn, Effects of surface modification on rheological and mechanical properties of CNT/epoxy composites, Carbon, 44 (2006) 1898-1905.
[16] A.I. Isayev, R. Kumar, T.M. Lewis, Ultrasound assisted twin screw extrusion of polymer–nanocomposites containing carbon nanotubes, Polymer, 50 (2009) 250-260.
[17] Z. Špitalský, C.A. Krontiras, S.N. Georga, C. Galiotis, Effect of oxidation treatment of multiwalled carbon nanotubes on the mechanical and electrical properties of their epoxy composites, Composites Part A: Applied Science and Manufacturing, 40 (2009) 778-783.
[18] W. Li, D. He, Z. Dang, J. Bai, In situ damage sensing in the glass fabric reinforced epoxy composites containing CNT–Al2O3 hybrids, Composites Science and Technology, 99 (2014) 8-14.
[19] W. Li, D. He, J. Bai, The influence of nano/micro hybrid structure on the mechanical and self-sensing properties of carbon nanotube-microparticle reinforced epoxy matrix composite, Composites Part A: Applied Science and Manufacturing, 54 (2013) 28-36.
[20] H. Yang, S. Liu, L. Cao, S. Jiang, H. Hou, Superlithiation of non-conductive polyimide toward high-performance lithium-ion batteries, Journal of Materials Chemistry A, 6 (2018) 21216-21224.
[21] X. Liao, W. Ye, L. Chen, S. Jiang, G. Wang, L. Zhang, H. Hou, Flexible hdC-G reinforced polyimide composites with high dielectric permittivity, Composites Part A: Applied Science and Manufacturing, 101 (2017) 50-58.
[22] Y. Liu, Y. Xu, B. Fan, M. Yang, A.-L. Hamon, P. Haghi-Ashtiani, D. He, J. Bai, Constructing 3D CNTs-SiO2@RGO structures by using GO sheets as template, Chemical Physics Letters, 713 (2018) 189-193.
[23] Y. Liu, A.-L. Hamon, B. Fan, D. He, P. Haghi-Ashtiani, T. Reiss, J. Bai, Intensive EELS study of epoxy composites reinforced by graphene-based nanofillers, Journal of Applied Polymer Science, 135 (2018) 46748.
[24] I. Choi, J.G. Kim, D.G. Lee, I.S. Seo, Aramid/epoxy composites sandwich structures for low-observable radomes, Composites Science and Technology, 71 (2011) 1632-1638.
[25] M. Chen, Y. Pei, D. Fang, Design, fabrication, and characterization of lightweight and broadband microwave absorbing structure reinforced by two dimensional composite lattice, Applied Physics A, 108 (2012) 75-80.

[26] Z. Chen, C. Xu, C. Ma, W. Ren, H.-M. Cheng, Lightweight and Flexible Graphene Foam Composites for High-Performance Electromagnetic Interference Shielding, Advanced Materials, 25 (2013) 1296-1300.
[27] R. Shu, Z. Wan, J. Zhang, Y. Wu, Y. Liu, J. Shi, M. Zheng, Facile Design of Three-Dimensional Nitrogen-Doped Reduced Graphene Oxide/Multi-Walled Carbon Nanotube Composite Foams as Lightweight and Highly Efficient Microwave Absorbers, ACS Applied Materials & Interfaces, 12 (2020) 4689-4698.
[28] K.-Y. Park, S.-E. Lee, C.-G. Kim, J.-H. Han, Fabrication and electromagnetic characteristics of electromagnetic wave absorbing sandwich structures, Composites Science and Technology, 66 (2006) 576-584.
[29] Y. Chen, L. Sui, H. Fang, C. Ding, Z. Li, S. Jiang, H. Hou, Superior mechanical enhancement of epoxy composites reinforced by polyimide nanofibers via a vacuum-assisted hot-pressing, Composites Science and Technology, 174 (2019) 20-26.
[30] N. Belhadj-Tahar, A. Fourrier-Lamer, Broad-Band Analysis of a Coaxial Discontinuity Used for Dielectric Measurements, IEEE Transactions on Microwave Theory and Techniques, 34 (1986) 346-350.
[31] R.C. Thompson, Optical Waves in Layered Media, Journal of Modern Optics, 37 (1990) 147-148.
[32] P.A. Miles, W.B. Westphal, A. Von Hippel, Dielectric Spectroscopy of Ferromagnetic Semiconductors, Reviews of Modern Physics, 29 (1957) 279-307.
[33] J. Dong, W. Zhou, Y. Qing, L. Gao, S. Duan, F. Luo, D. Zhu, Dielectric and microwave absorption properties of CB doped SiO2f/PI double-layer composites, Ceramics International, 44 (2018) 14007-14012.
[34] Y.-W. Nam, J.-H. Choi, W.-J. Lee, C.-G. Kim, Thin and lightweight radar-absorbing structure containing glass fabric coated with silver by sputtering, Composite Structures, 160 (2017) 1171-1177.
[35] H. Wang, D. Zhu, Double layered radar absorbing structures of Silicon Carbide fibers/polyimide composites, Synthetic Metals, 246 (2018) 213-219.